LA-UR -83-875

Los Alamos National Laboratory is operated by the University of California for the United States Department of Energy under contract W-7405-ENG-36.

LA-UR--83-875

DE83 009866

TITLE: AN INTRODUCTION TO MULTIDIMENSIONAL COMBUSTION MODELING WITH THE CONCHAS-SPRAY COMPUTER PROGRAM

AUTHOR(S): Peter J. O'Rourke

SUBMITTED TO: Workshop on Nonlinear Problems in Applied Combustion, Rocquencourt France, December 7-10, 1982

DISCLAIMER

Los Alamos Los Alamos National Laboratory
Los Alamos, New Mexico 87545

FORM NO 836 R4
ST NO 2629 5/81

MASTER

AN INTRODUCTION TO MULTIDIMENSIONAL COMBUSTION MODELING WITH THE CONCHAS-SPRAY COMPUTER PROGRAM

P. J. O'Rourke
Theoretical Division, Group T-3
University of California
Los Alamos National Laboratory
Los Alamos, NM 87545

ABSTRACT

CONCHAS-SPRAY is a finite-difference computer code for the calculation of two-dimensional chemically reacting fluid flows. In this paper we discuss four problem areas that are encountered in multidimensional numerical combustion modeling, and the numerical techniques used by CONCHAS-SPRAY to overcome these problems. Then the equations are given that are solved by the computer code, and some results from an example problem are discussed.

INTRODUCTION

In 1975, Group T-3 of Los Alamos National Laboratory was asked by the Department of Energy to develop a multidimensional numerical model for the fluid flow and combustion in an internal combustion engine cylinder. One fruition of this effort is the CONCHAS-SPRAY computer program.[1] CONCHAS-SPRAY solves by finite-difference techniques the unsteady equations for a multi-component, chemically reacting mixture of ideal gases, together with those for an evaporating liquid spray. The geometry is spatially two-dimensional and can be either planar or axisymmetric. In the latter case, the equation for the azimuthal (swirl) velocity component is solved. Although the program is written for internal combustion engine applications, with little modification it can be used for a variety of other combustion problems. For example, CONCHAS-SPRAY is currently being used to simulate the combustion of hydrogen-air mixtures in large containment vessels.[2]

This paper is intended as an introduction to the CONCHAS-SPRAY program. We will describe four problem areas that are encountered in internal combustion engine modeling. These are that one must calculate in complicated geometries, calculate low Mach number flows with large density var ations, calculate the flame speeds of thin flames, and calculate the dynamics of vaporizing liquid fuel sprays. For eac. of these areas, we will describe what the problem is and the numerical techniques that have been used to overcome it. The last two techniques have been developed directly as a result of our involvement in the internal combustion engine program, and these will be described in more detail. All four problems share the common characteristic that they are only problems in multidimensional combustion modeling. We will describe why these problems either are not encountered or are easily dealt with in one-dimensional geometries. After describing the four problem areas, we will give the equations that are solved by CONCHAS-SPRAY and present some results from an example solution.

Because we will discuss four problems does not mean that there are not many more problem areas to be dealt with in internal combustion engine modeling. A listing of some of these outstanding problem areas follows.

1. Turbulence Modeling. The combustion in internal combustion engines occurs in a turbulent fluid. How detailed should our turbulence transport model be, and what type of averaging should be used to obtain the turbulence equations?
2. Chemical Rate Equations. Due to computer time limitations, in a multidimensional calculation one must use simplified, global chemical reactions. How should one choose these global reactions and their rates? The method of high activation energy asymptotics could provide an answer to this difficult question.[3]

3. Turbulent Flame Structure. What is the structure of the turbulent flames in engines? How should we calculate turbulent flames and their speeds.
4. Wall Heat Loss. Wall heat loss is known to have a significant effect on engine performance.[4] Do present wall-heat-loss models adequately predict this effect?
5. Thick Spray Effects. In engine sprays, a large class of effects, sometimes called "thick spray" effects,[5] are known to occur. Among these are drop collisions, oscillations, and the break-up into droplets of ligaments that persist downstream of the atomizer. Only recently has a method been developed to calculate drop collisions,[6] and the remaining effects are largely neglected in current spray models.

For all of these problem areas we have adopted preliminary models that must be tested and refined in careful comparisons with laboratory experiments.

Problem 1

Computing in Complicated Geometries

Shown in Fig. 1 is one design for a stratified charge engine cylinder[7] that is being considered by the General Motors Corporation. The spray is injected axisymmetrically at the cylinder head, and the cup in the piston and small clearance at top-dead-center between piston and cylinder head, are designed to produce a fluid flow that optimizes charge stratification and rapid combustion. The geometry is a challenging one for numerical modellers. In addition to the complicated boundary shape, the boundary is moving.

Until ten years ago, fluid dynamics calculations could not be routinely performed in such a complicated geometry. Older solution procedures are divided

into two classes: Eulerian methods and Lagrangian methods. In Eulerian methods the computational mesh is fixed in the laboratory frame, and thus the computing region has to have a fixed shape. Lagrangian methods, in which the computational mesh moves with the fluid, can only calculate flows with small fluid distortions, because large fluid distortions produce large mesh distortions and give rise to intolerable numerical errors. CONCHAS-SPRAY utilizes the Arbitrary-Lagrangian-Eulerian or ALE method.[8] In this method, the computational mesh is composed of arbitrary quadrilaterals that can move in any manner relative to the fluid. In an engine calculation the mesh can move to follow the piston motion.

Figure 2 shows a possible computational cell V_{ij} in an ALE mesh. In computer memory are kept the values of the thermodynamic variables, which are located at the center of the cell, and the positions and velocities of the cell vertices. In the course of a computational cycle, these quantities are updated in time by the computational time step δt. The finite-difference equations that are used to accomplish this can be viewed as approximations to the integral balance equations for mass, momentum, and energy over the control volume V_{ij}. Strict conservation of mass and momentum is observed in the finite-difference formulations. An internal energy equation is solved by CONCHAS-SPRAY, and those terms that are in conservative form in this equation are differenced conservatively.

Problem 2

Computing Low Mach Number Flows with Large Density Variations

In most combustion problems, the Mach numbers associated with the flow are much smaller than one. When this is true, although it is changing in time one can show that the pressure is nearly uniform in space.[9] Unlike the low Mach num-

ber flows that we are most accustomed to, in which the density is constant in space, the density can vary by a factor of six or seven in space in combustion problems.

Again, until about ten years ago, such flows could not be calculated with existing numerical methods. Older methods are divided into two classes[10]: stream function and vorticity methods and compressible flow methods in which the Courant condition $\frac{(|\underline{u}| + c)\delta t}{\delta x} < 1$ has to be observed. Here $\underline{u}$ is the flow velocity and c the adiabatic speed of sound. Stream function methods cannot be used because no stream function exists in combustion problems. A stream functon $\underline{\psi}$ satisfies $\underline{u} = \nabla \times \underline{\psi}$, but this implies that $\nabla \cdot \underline{u} = 0$. $\nabla \cdot \underline{u}$ is the fractional rate of change of volume of a fluid element, and in combustion problems $\nabla \cdot \underline{u} \neq 0$ due to chemical heat release and a heat flux vector whose divergence is locally large. Traditional compressible flow methods, which require satisfying the Courant condition, can be used in combustion problems, but when the Mach number is small, they are extremely inefficient. When one observes the Courant condition, the computational time step is small enough to resolve the acoustic wave motion in the combustion chamber. But these occur on a time scale t_c that is much smaller than time scales of interest t_u, which are those associated with convective motion. The ratio t_c/t_u is the Mach number. Thus an extremely large number of time steps is needed to calculate for problem times of interest in low Mach number flows.

CONCHAS-SPRAY utilizes the ICE (Implicit Continuous-Fluid Eulerian) method,[11] which eliminates the need to observe the Courant condition on the computational time step. Although the ICE method was originally developed for Eulerian codes and referred to a specific set of finite-difference equations, the name ICE

is now generally applied to any fluid flow algorithm with the following two features: the linear momentum equations are solved (rather than the vorticity equation(s)) and implicit finite differencing is used for those terms associated with acoustic or pressure wave motions. These terms are the pressure gradient terms in the momentum equations and the dilation ($\nabla \cdot \underline{u}$) terms in the mass and energy equations. Because of this implicit differencing, the same numerical algorithm can be used to calculate efficiently flows with any Mach number. In the low Mach number limit, the algorithm reduces to one that solves low Mach number equations, in which the pressure is uniform.

Since the ICE method can be used to calculate flows of any Mach number, it is natural to ask whether one might sacrifice some of this capability and save additional computer time by solving equations that are specifically formulated for low Mach number flows. Such formulations are available[9,12] for chemically-reacting flows; however, in more than one space dimension, these low Mach number equations are nearly as complicated as the general equations for compressible flows, and no computational time can be saved by using them. In one space dimension, it is well known[13] that for most practical purposes one need not solve the momentum equation in combustion problems. This is a significant simplification that allows one to save much computer time. In more than one space dimension, however, when one dispenses with the momentum equations, essential information has been lost.

Problem 3

Calculating the Speeds of Thin Flames

The problem is simply that laminar flames and some turbulent flames have thicknesses that are smaller than the computational cell sizes that one can af-

ford to use in multidimensional calculations. We will first describe briefly the numerical methods that have been proposed for solving this problem, and then we will give the method used in CONCHAS-SPRAY, which is an artificial flame thickening procedure.[9]

Thin flame calculation strategies can be divided into three classes: adaptive gridding, discontinuous flame modeling, and artificial flame thickening. Adaptive grid strategies can, in turn, be placed in two categories. These are illustrated in Fig. 3. In the first category, there are those strategies in which the computational mesh is fixed, but some cells are subdivided to provide more resolution where gradients are larger. In contrast, in the second category the number of computational cells is fixed, but the cells move and become smaller in regions of large gradients. Although there have been some notable successes in particular problems with second category strategies,[14] both strategies need further development before they can be more universally and reliably applied to multidimensional combustion modeling. We remark that in one-dimensional problems second category strategies are fairly easy to implement in CONCHAS-SPRAY.

A second flame resolution strategy is to treat the flame as a discontinuity with a prescribed flame velocity relative to the fluid ahead of the discontinuity. Numerical methods for convecting a material interfaces are highly developed.[15,16] The new element in flame modeling is that the interface moves relative to the fluid ahead of it. A method for accomplishing this, using Huyghens principle, has been developed by Chorin.[17] The flame speed can be prescribed using the result of analytic solutions, experimental data, or subsidiary one-dimensional calculations. This second flame resolution strategy is a viable alternative to the method we presently use.

The method we use to resolve thin flames is to artifically thicken the flame to dimensions that are resolvable by the computational mesh.[9,18] This is accomplished without changing the flame speed. The method is easy to implement. One simply multiplies the mass, momentum, and energy diffusivities by a factor β, divides the reaction rates by β, and uses these scaled values in the calculation. β can be a function of space and time. The effect of this transformation increase the computed flame thickness by a factor of β. Thus, little computer programming is required to implement the method, and flames are automatically thickened whenever and wherever they occur in a calculation.

The spirit of the artificial flame thickening method is similar to that of classical shock smearing.[19] There is a big difference, however, between computing thickened shocks and thickened flames. In computing shocks, the correct shock speed is obtained as long as one conserves mass, momentum, and energy in the finite-difference equations and uses the correct boundary conditions. In most applications, the detailed shock structure need not be resolved. In contrast, to calculate the correct flame speed, one must resolve the detailed flame structure. Fortunately, it has been our experience that for the simple flame structures we have calculated, in which there is a one-step chemical reaction taking fuel and oxygen to products, three or four cells are sufficient to resolve the flame and obtain the correct flame speed.

Problem 4

Fuel Spray Modeling

To calculate the essential dynamics of a vaporizing fuel spray, one needs to include the effects of a distribution of drop sizes, velocities, and temperatures. Thus one must solve what is called[20] the "spray equation:"

$$\frac{\partial f}{\partial t} + \nabla_{\underline{x}} \cdot (f\underline{v}) + \nabla_{\underline{v}} \cdot (f\underline{F}) + \frac{\partial}{\partial r}(fR) + \frac{\partial}{\partial T_d}(f\dot{T}_d) = 0 \quad . \tag{1}$$

This is a stochastic equation for the probability distribution f of drop positions $\underline{x}$, velocities $\underline{v}$, radii r, and temperatures T_d. $\underline{F}$ is the drop acceleration, R is the rate of drop radius change, and $\dot{T}_d$ is the rate of drop temperature change. We have given here a simple form of the spray equation that expresses conservation of drop numbers in volumes that move with the drop velocities in a hyperspace, called "drop-space," whose coordinates are ($\underline{x}$, $\underline{v}$, r, T_d). In more complicated forms of the equation, there are source terms on the right-hand-side of (1) due to the turbulent transport of drops, collisions, or break-ups. The basic problem of fuel spray modeling is that Eq. (1), in conjunction with the gas-phase equations, is very difficult to solve. Three methods have been proposed for numerically solving the coupled spray and gas-phase equations: direct solution methods, moment equation methods, and parcel methods. We now describe the three methods and tell why we use a parcel method in CONCHAS-SPRAY.

In direct solution methods, one subdivides drop-space into computational cells, in each of which a value of f is stored. The values of f are updated in time by approximating (1) by finite-differences. The problem with direct solution methods is that computer storage requirements are excessive in multidimensional calculations. In problems with two space dimensions, drop space is six dimensional, and if one uses ten cells to resolve each coordinate direction in drop space, then there will be a total of 10^6 computational cells. This much storage is available on the largest of today's computers, but with the addition of more dimensions to drop-space, such as a swirl velocity component as we have in CONCHAS-SPRAY, or when more resolution is required, computer storage is exceeded.

In moment equation methods, one reduces the number of independent variables by integrating Eq. (1) over one or more coordinates of drop-space. Usually (1)

is multiplied by functions of $\underline{v}$, r, and T_d and integrated over these same coordinates, and usually only mass, momentum, and energy equations are used for the spray.[21] These moment equations contain terms which give the total exchange rates of mass, momentum, and energy between the two phases.

The problem with moment equation methods is that these exchange rates are difficult to evaluate accurately. In order to calculate the exchange rates, one needs to know the distribution function f, and accurate approximations to f cannot be constructed from the small number of moments of f that are known.

In CONCHAS-SPRAY, we use a stochastic parcel method developed by Dukowicz.[22] The spray is represented by computational parcels, each parcel being composed of a number of drops of identical size, velocity, and temperature. There is a stochastic sampling of the assumed probability distribution of drop properties at injection and of the distributions governing drop behavior at downstream locations. An additional feature of the method is that drop and gas accelerations are calculated by an implicit scheme that circumvents time-step limitations due to the close-coupling of drop and gas velocities. The distribution function f is obtained by ensemble-averaging over many calculations in an unsteady problem or by time-averaging in a steady problem.

In practice, it is found that with less than one thousand parcels, computational results are obtained that do not change when one uses different random number sequences to generate the results. One reason for the economy of parcel methods is that since parcels follow drop trajectories, the parcels move where the drops move, automatically providing more resolution (i.e. more parcels) where it is needed.

The CONCHAS-SPRAY Equations

In this section we give the equations solved by CONCHAS-SPRAY and briefly describe some of the terms. The equations are given in vector notation. The spray equation has already been given, and we suppy here the forms used for the rates of drops velocity, radius, and temperature change. The symbols are defind in Table I.

Continuity Equation for Species K

$$\frac{\partial \rho_k}{\partial t} + \underline{\nabla}\cdot(\rho_k \underline{u}) = \underline{\nabla}\cdot\left[\rho D \underline{\nabla}\left(\frac{\rho_k}{\rho}\right)\right] + W_k \sum_r (b_{k,r} - a_{k,r})\dot{\omega}_r$$

$$- \delta_{k,\ell} \iiint f\, 4\pi r^2 R \rho_\ell \, dr \, d\underline{v} \, dT_d \qquad (2)$$

$$\rho = \sum_k \rho_k$$

Momentum Equations

$$\frac{\partial \rho \underline{u}}{\partial t} + \underline{\nabla}\cdot(\rho \underline{u}\underline{u}) + \underline{\nabla} p = \underline{\nabla}\cdot\underline{\underline{\sigma}} + \rho \underline{g} - \iiint f \rho_\ell \left[4\pi r^2 R \underline{v} + \frac{4}{3}\pi r^3 \underline{F}\right] dr \, d\underline{v} \, dT_d$$

$$\underline{\underline{\sigma}} = \mu[\underline{\nabla u} + (\underline{\nabla u})^T]\underline{\nabla}\cdot\underline{u}\ \underline{\underline{I}} - \frac{2}{3}\mu\, \underline{\nabla}\cdot\underline{u}\ \underline{\underline{I}} \qquad (3)$$

Internal Energy Equation

$$\frac{\partial \rho I}{\partial t} + \underline{\nabla}\cdot(\rho \underline{u} I) + p \underline{\nabla}\cdot\underline{u} = \underline{\underline{\sigma}} : \underline{\nabla u} + \underline{\nabla}\cdot\left[K \underline{\nabla} T + \rho D \sum_k h_k \underline{\nabla}\left(\frac{\rho_k}{\rho}\right)\right] + \sum_r \dot{\omega}_r q_r$$

$$- \iiint f \rho_\ell \{4\pi r^2 \sigma h_\ell(T_d) + \frac{1}{2}(\underline{v} - \underline{u})^2] \qquad (4)$$

$$+ \frac{4}{3}\pi r^3 [c_\ell \dot{T}_d + \underline{F}\cdot(\underline{v} - \underline{u})]\} \, dr \, d\underline{v} \, dT_d$$

$$q_r = - \sum_k (b_{k,r} - a_{k,r}) h_{k,o}$$

Equations of State

$$p = RT \sum_k \left(\frac{\rho_k}{W_k}\right)$$

$$I(T) = \sum_k \left(\frac{\rho_k}{\rho}\right) I_k(T) \qquad (5)$$

Transport Coefficients

$$\mu = \mu_t + \mu_o$$

$$\mu_o = \rho \nu_o \text{ where } \nu_o = \text{constant}$$

$$\mu_t = \frac{1}{\sqrt{2}} \rho K_D^2 \Lambda^2 (\underline{\underline{D}} \cdot \underline{\underline{D}})^{\frac{1}{2}}$$

$$\underline{\underline{D}} = \frac{1}{2} \left(\nabla \underline{u} + (\nabla \underline{u})^T\right) \qquad (6)$$

$$Sc = \frac{\mu}{\rho D} = \text{constant}$$

$$Pr = \frac{\mu c_p}{k} = \text{constant}$$

Chemical Rate Equations

Kinetic Reactions

$$\dot{\omega}_r = K_{f,r}(T) \prod_k \left(\frac{\rho_k}{W_k}\right)^{a'_{k,r}} - K_{b,r}(T) \prod_k \left(\frac{\rho_k}{W_k}\right)^{b'_{k,r}} \qquad (7a)$$

Equilibrium Reactions

$$\prod_k \left(\frac{\rho_k}{W_k}\right)^{b_{k,r}-a_{k,r}} = K_{c,r}(T) \tag{7b}$$

Rates of Drop Velocity, Size, and Temperature Change

$$\underline{F} = \frac{3}{8}\frac{\rho}{\rho_\ell}\frac{|\underline{u} - \underline{v}|}{r}(\underline{u} - \underline{v})C_D + \underline{g}$$

$$R = -\frac{\lambda}{2\rho_\ell c_p r}\frac{Y_1^* - Y_1}{1 - Y_1^*}\,Sh \tag{8}$$

$$\frac{4}{3}\pi r^3 c_\ell \dot{T}_d = L(T_d)4\pi r^2 R + Q$$

$$Q = 2\pi r\,\lambda(T - T_d)Nu$$

The continuity equation for species k has convection, turbulent diffusion, and chemical reaction terms. In addition, species 1, which is the vapor phase of the liquid fuel, has a source term due to vaporization of the spray. This has the form of a sum over all drops of the rate of mass loss of each drop. The liquid density ρ_ℓ is assumed to be constant in time and space. The momentum equation (3) has convection, pressure gradient, turbulent stress, and body force terms, and a source term due to momentum exchange with the spray. The latter has the form of a sum over all drops of the rate of momentum loss of each drop. The turbulent stress tensor is assumed to be Newtonian in form.

An internal energy equation is solved by CONCHAS-SPRAY. "I" is the specific internal energy of the gas mixture relative to zero internal energy at absolute

zero. This equation has terms due to convection, pressure work, dissipation due to the turbulent stress, turbulent heat flux, chemical heat release, and energy exchange with the spray.

The equations of state are those for a mixture of ideal gases, and the species internal energies are obtained from the JANNAF[23] thermochemical tables. The viscosity coefficient μ is the sum of contributions from a constant diffusivity ν_o and a sub-grid scale turbulent viscosity μ_t.[24]

Chemical reactions are divided into two classes: kinetic reactions, whose rates are explicitly prescribed, and equilibrium reactions for which the rate of change of the reaction progress variable $\dot{\omega}_r$ is determined implicitly by an equilibrium constraint. An Arrhenius law temperature dependence is used for the rates of kinetic reactions.

A drag coefficient C_D correlation is used to determine the rate of change of drop velocity $\underline{F}$. The rate of drop radius change $\dot{R}$ is the product of a Sherwood number Sh and the value $\dot{R}$ would have if the drop were vaporizing in spherically-symmetric surroundings. Y_1^* is the fuel vapor mass fraction at the drop's surface and is found from the surface equilibrium approximation.[13] The heat transfer to each drop Q is determined from a Nusselt number Nu correlation. Finally, the rate of drop temperature change $\dot{T}_d$ is determined from an energy equation for the drop. It is assumed that the drop temperature T_d is uniform within each drop. The precise correlations used for C_d, Sh, and Nu are given in Ref. 1.

A Computational Example

We now give a some of the results from a CONCHAS-SPRAY calculation of a typical compression and power stroke for the stratified charge engine of Fig. 1. So much information is available that to describe all the results from such a calculation would require a paper in itself. Our intent here is only to indicate the

detailed nature of the information obtainable from such a calculation, to show the care that must be exercised in interpreting the results, and to emphasize the preliminary nature of the numerical model.

Figure 4 shows the computational mesh at the beginning of the calculation. The left boundary is the axis of symmetry; the top boundary is the cylinder head; the right boundary is the cylinder wall; and the bottom boundary shows the outline of the piston with its chamfered bowl. The distance between the cylinder head and top of the piston is 9.7 cm. The computational region is resolved with 20 cells in the radial direction and 32 cells in the axial direction. Some of the cells in the lower right hand corner of the mesh do not appear in the plot. These are obstacle cells that do not participate in the calculation.

The calculation was begun at a crank angle of 180° before top-dead-center (TDC). Until 52° before TDC the gas in the cylinder was compressed by the upward piston motion. Between 52° and 39° before TDC a liquid octane spray was injected into and vaporized in the compressionally heated cylinder gases. At 27° before TDC spark ignition was simulated by depositing energy in one computational cell near the cylinder head and symmetry axis, and at TDC most of the fuel had been burned. The calculation was terminated at 180° after TDC. The total problem time was 37.5 ms, corresponding to an engine speed of 1600 rpm. The total computational time was 45 minutes on a CRAY I computer.

The fuel in this calculation was consumed by the single-step irreversible chemical reaction:

$$2C_8H_{18} + 25O_2 \xrightarrow{\dot{\omega}_r} 16CO_2 + 18H_2O \quad .$$

Subsequently, the local chemical equilibrium composition was calculated of a mixture of CO_2, H_2O, and their dissociation products.

At user-selected output intervals the computer program plotted the computational mesh, velocity vectors, spray parcel positions, and contour plots of several flow quantities. Figures 5, 6, and 7 show some plots from the above calculation at 22° before TDC, when burning is still occurring. Figure 5 shows the computational mesh and the spray parcel plot; Fig. 6 gives plots of the temperature and fuel vapor mass fractions; in Fig. 7 are shown plots of the mass fraction of diatomic oxygen (O_2) and the equivalence ratio ϕ. (The equivalence ratio ϕ is defined by $\phi = R/R_{st}$, where R is the ratio of the molar concentration of fuel vapor to that of O_2 and R_{st} is the stoichiometric value of R.)

The plot of the computational mesh shows the manner in which the mesh has been moved. Comparison with the plot of Fig. 4 shows that those cells in the pison cup have retained their original shape and have been simply translated upward with the piston velocity. Those cells above the top of the piston have retained their original radial dimension but have been compressed uniformly in size in the axial direction. In addition, some rows of cells above the piston have been deleted for economy.

The spray parcel plot of Fig. 5 shows that many unevaporated liquid drops remain in the cylinder. Comparison with the temperature plot of Fig. 6 shows that these drops reside in the cooler regions of the cylinder, and Fig. 5 shows that some of these drops have impinged on the piston wall. When this occurs, the spray parcel positions are held fixed in the calculation, and the drops are evaporated using drop vaporization rates for the gas-phase conditions of the cell in which they are located. If an appreciable amount of liquid were to impinge on the wall or if we were concerned with calculating trace amounts of unburned hydrocarbon gases, a more accurate model would have to be used for the vaporization of a liquid film on a wall.

At first glance, the temperature contour plot of Fig. 6 seems to show a premixed flame front surrounding a hot kernel of gases near the location of ignition. The situation is much more complicated, however, as is revealed by an examination of the fuel vapor, oxygen, and equivalence ratio plots. In the center of the kernel of hot gases there is little or no oxygen. To the right of the kernel there is oxygen and no fuel. Thus the temperature gradients to the right of the hot kernel are not indicative of a premixed flame, but merely separate a hot, fuel-rich region from a cool, oxygen-rich one. There is some diffusion flame burning here.

At the bottom of the hot kernel, the temperature gradients are steeper. The equivalence ratio plot shows that the mixture below the hot kernel is nearly stoichiometric, and the fuel concentration plot shows all the fuel being depleted in this region. The steep temperature gradients here are thus associated with rapid, premixed burning.

The temperature gradients to the left of the hot kernel are also associated with a premixed flame, but here the flame is propagating into a region whose equivalence ratio is 4.5. Due to the low oxygen concentration here, chemical reaction is slower, and the competition of the slow chemical reaction with turbulent heat and mass diffusion results in a slower, thicker flame than at the bottom of the kernel. In addition as the flame on the left passes over the unburned mixture, all the oxygen is consumed, leaving hot, fuel-laden gases.

It is, of course, physically unrealistic to have unburned octane present in a region with temperatures higher than 2000 K. In reality, when a premixed flame passes over a region of equivalence ratio $\phi > 1$, all the fuel reacts, and the mixture behind the flame contains partially oxidized combustion products that are

nearly in chemical equilibrium. The fault here lies with our chemical kinetics model in which the fuel can only directly react to form complete combustion products. We are currently looking at improved chemical kinetics models that overcome this difficulty.[25]

Despite this and other known difficulties with the model, it can predict in-cylinder pressure histories with reasonable accuracy, as well as the correct trends in pressure change with changes in operating conditions.[26,27] Thus CONCHAS-SPRAY is currently a useful design tool for automobile manufacturers and research tool for many combustion problems.

Acknowledgment

The author wishes to thank A. A. Amsden, who performed the example calculation; researchers at General Motors Corporation for supplying the operating conditions for our example; and T. D. Butler, J. D. Ramshaw, J. K. Dukowicz, and L. D. Cloutman for help in preparing this manuscript.

References

1. L. D. Cloutman, J. K. Dukowicz, J. D. Ramshaw, and A. A. Amsden, "CONCHAS-SPRAY: A Computer Code for Reactive Flows with Fuel Sprays," Los Alamos National Laboratory report LA-9294-MS (May 1982).

2. P. J. O'Rourke, "Numerical Calculations of the Bouyant Combustion of Hydrogen-Air Mixtures," to be published as a Los Alamos National Laboratory Mini-review.

3. P. C. Fife and B. Nicolaenko, "Asymptotic Flame Theory with Complex Chemistry," Los Alamos National Laboratory report LA-UR-82-2993 (To appear in the Proceedings of Special Summer Conference on Partial Differential Equations, Durham, N.H., June 1982).

4. F. V. Bracco, "Modeling of Two-Phase, Two Dimensional, Unsteady Combustion for Internal Combustion Engines," Proc. of the Institution of Mechanical Engineers International Conference on Stratified Charge Engines, London (1976).

5. F. V. Bracco, "Introducing a New Generation of More Detailed and Informative Combustion Models," SAE Transactions, 84, 3317 (1975).

5. F. V. Bracco, "Introducing a New Generation of More Detailed and Informative Combustion Models," SAE Transactions, 84, 3317 (1975).

6. P. J. O'Rourke, "Collective Drop Effects and Vaporizing Liquid Sprays," Los Alamos National Laboratory report LA-9069-T (1981).

7. F. V. Bracco, "Toward an Optimal Automotive Power Plant," Comb. Sci. Tech, 12, 1 (1976).

8. C. W. Hirt, "An Arbitrary Lagrangian-Eulerian Computing Technique," Proc. Int. Conf. Numer. Methods Fluid Dyn. 2nd, Berkerely, Cal. (1970).

9. P. J. O'Rourke and F. V. Bracco, "Two Scaling Transformations for the Numerical Computation of Multidimensional Unsteady Laminar Flames," J. Comput. Phys. 33, 2, 185 (1979).

10. P. J. Roache, Computational Fluid Dynamics (Hermosa Publishers, Albuquerque, N.M., 1972).

11. F. H. Harlow and A. A. Amsden, "A Numerical Fluid Dynamics Calculation Method for All Flow Speeds," J. Comput. Phys., 8, 2, 197.

12. J. D. Ramshaw and J. A. Trapp, "A Numerical Technique for Low-Speed Homogeneous Two-Phase Flow with Sharp Interfaces," J. Comput. Phys. 21, 4, 438.

13. F. A. Williams, Combustion Theory (Addison-Wesley Publishing Company, Inc., Reading, Mass., 1965).

14. J. Saltzman, "A Variational Method for Generating Multidimensional Adaptive Grids," Courant Mathematics and Computing Report DOE/ER/03077-174, New York University (1982).

15. C. W. Hirt and B. D. Nichols, "Volume of Fluid (VOF) Method for the Dynamics of Free Boundaries," J. Comput. Phys. 39, 201 (1981).

16. W. F. Noh and P. Woodward, "SLIC (Simple Line Interface-Calculation)," in Proc. Int. Conf. Numer. Methods Fluid Dyn. 5th, Enschede, Netherlands (1976).

17. A. J. Chorin, "Flame Advection and Propagation Algorithms," J. Comput. Phys. 35, 1, 1 (1980).

18. T. D. Butler and P. J. O'Rourke, "A Numerical Method for Two-Dimensional Unsteady Reacting Flows," Proc. Sixteenth Int. Symp. on Combustion, The Combustion Institute (1977).

19. J. von Neumann and R. D. Richtmyer, "A Method for the Numerical Calculation of Hydrodynamic Shocks," J. Appl. Phys. 21, 232 (1950).

20. F. A. Williams, "Progress in Spray-Combustion Analysis," Proc. Eighth Int. Symp. on Combustion, The Combustion Institute (1962).

20. F. A. Williams, "Progress in Spray-Combustion Analysis," Proc. Eighth Int. Symp. on Combustion, The Combustion Institute (1962).

21. J. R. Travis, F. H. Harlow, and A. A. Amsden, "Numerical Calculation of Two-Phase Flows," Nucl. Sci. Engr. 61, 1-10 (1976).

22. J. K. Dukowicz, "A Particle-Fluid Numerical Model for Liquid Sprays," J. Comput. Phys. 35, 2, 229 (1980).

23. D. R. Stull and H. Prophet, "JANAF Thermochemical Table," 2nd Ed. (U.S. Department of Commerce/National Bureau of Standards, NSRDS-NBS 37, June 1971); M. W. Chase, et al., J. Phys. Chem. Ref. Data 3, 311 (1974).

24. J. W. Deardorff, "On the Magnitude of the Subgrid Scale Eddy Coefficient," J. Comput. Phys. 7, 120 (1971).

25. R. D. Reitz and F. V. Bracco, "Global Kinetics Models and Thermodynamic Equilibrium," submitted to Combustion and Flame.

26. S. H. El Tahry, "A Numerical Study on the Effects of Fluid Motion at Inlet-Valve Closure on Subsequent Fluid Motion in a Motored Engine," SAE Technical Paper Series 820035, Feb. 1982.

27. R. Diwalker, "Multidimensional Modeling Applied to the Direct-Injection Stratified Charge Engine--Calculation Versus Experiment," SAE Technical Paper Series 810225, Feb. 1981.

Table I

List of Symbols

Symbols	Definition
$a_{k,r}$, $b_{k,r}$	Forward and backward stoichiometric coefficients of species k in reaction r
$a'_{k,r}$, $b'_{k,r}$	Orders of the forward and backward reactions r with respect to species k
c_D	Droplet drag coefficient
c_ℓ	Specific heat of the liquid fuel
c_p	Gas specific heat at constant pressure
D	Turbulent mass diffusion coefficient
$\underline{\underline{D}}$	Rate-of-strain tensor
f	Droplet distribution function
$\underline{F}$	Droplet acceleration
$\underline{g}$	Acceleration due to gravity
h_k	Enthalphy of species k
h_{k_o}	Heat of formation of species k at absolute zero
h_ℓ	Liquid fuel enthalpy
I	Internal energy
$\underline{\underline{I}}$	Identity tensor
K	Turbulent heat transfer coeffient
$K_{c,r}$	Equilibrium constant for concentrations of equilibrium reaction r
K_D	Dimensionless coefficient in subgrid scale turbulent viscosity

Table I (continue)

Symbols	Definition
$K_{f,r}$, $K_{b,r}$	Forward and backward temperature dependencies of reaction r
L	Latent heat of vaporization of the fuel
μ_{l}	Droplet Nusselt number
p	Gas static pressure
q_r	Heat release of reaction r
Q	Heat transfer rate to a droplet
r	Droplet radius
R	Rate of droplet radius change
Sh	Droplet Sherwood number
t	Time
T	Gas temperature
T_d	Droplet temperature
$\dot{T}_d$	Rate of droplet temperature change
$\underline{u}$	Gas velocity
$\underline{v}$	Droplet velocity
W_K	Molecular weight of species K
Y_1	Mass fraction of gas species 1 (fuel vapor)
Y_1^*	Mass fraction of fuel vapor at a drop's surface
Λ	Length scale used in calculating subgrid scale turbulent viscosity
δ	Dirac delta function
λ	Gas molecular heat conduction coefficient
μ	Gas turbulent viscosity coefficient

Table I (continue)

Symbols	Definition
μ_t	Subgrid scale turbulent viscosity
μ_o	Turbulent viscosity due to constant diffusivity ν_o
ρ	Gas density
ρ_k	Density of gas species k
ρ_ℓ	Liquid fuel density
$\underline{\underline{\tau}}$	Turbulent stress tensor
$\dot{\omega}_r$	Reaction rate of reaction r

Figure Captions

Fig. 1. Stratified charge engine cylinder with a chamfered bowl in the piston.

Fig. 2. Computational cell in an ALE mesh and the locations of some of the cell variables.

Fig. 3. Adaptive mesh strategies. Top: Subdividing a fixed mesh. Bottom: Moving the mesh.

Fig. 4. Initial CONCHAS computational mesh in the example calculation.

Fig. 5. Computational mesh (top) and spray parcel positions (bottom) at 22° before TDC in the example calculation.

Fig. 6. Contours of fuel vapor mass fraction (top) and temperature (bottom) at 22° before TDC in the example calculation.

Fig. 7. Contours of oxygen mass fraction (top) and equivalence ratio (bottom) at 22° before TDC in the example calculation.

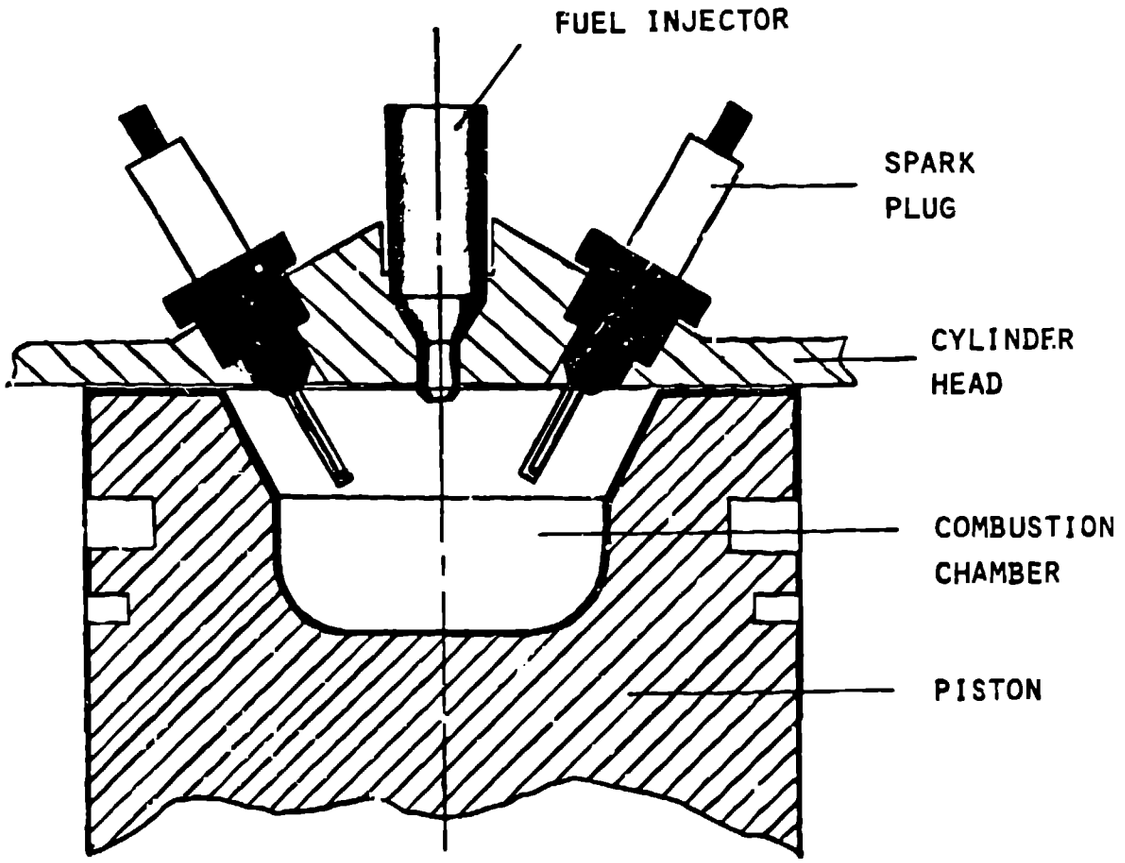
FUEL INJECTOR
SPARK
PLUG
CYLINDER
HEAD
COMBUSTION
CHAMBER
PISTON

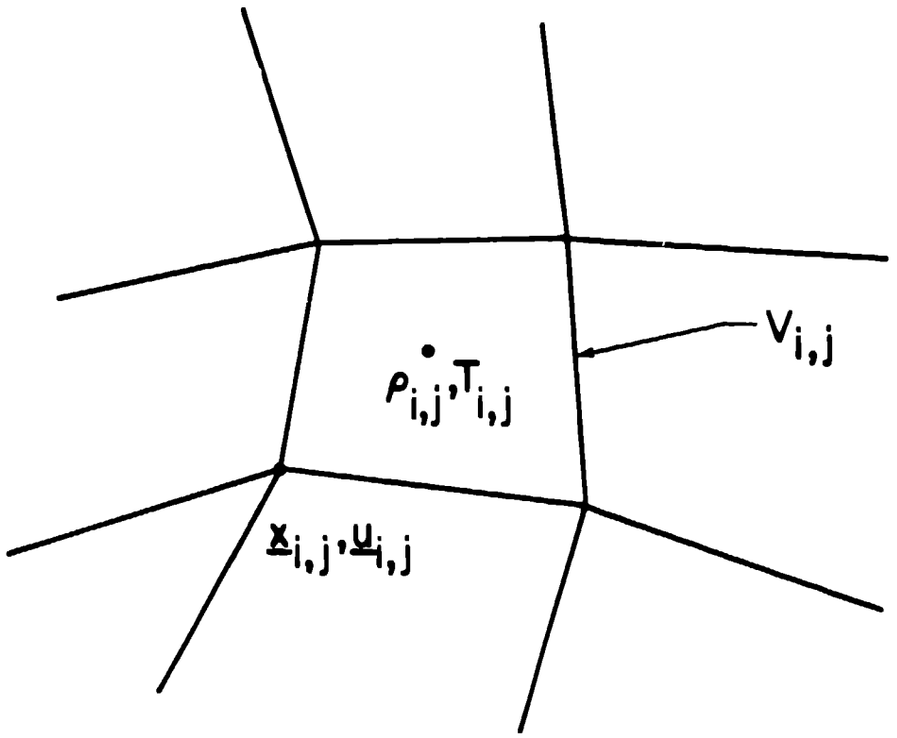
$V_{i,j}$
$\rho_{i,j}, T_{i,j}$
$x_{i,j}, y_{i,j}$

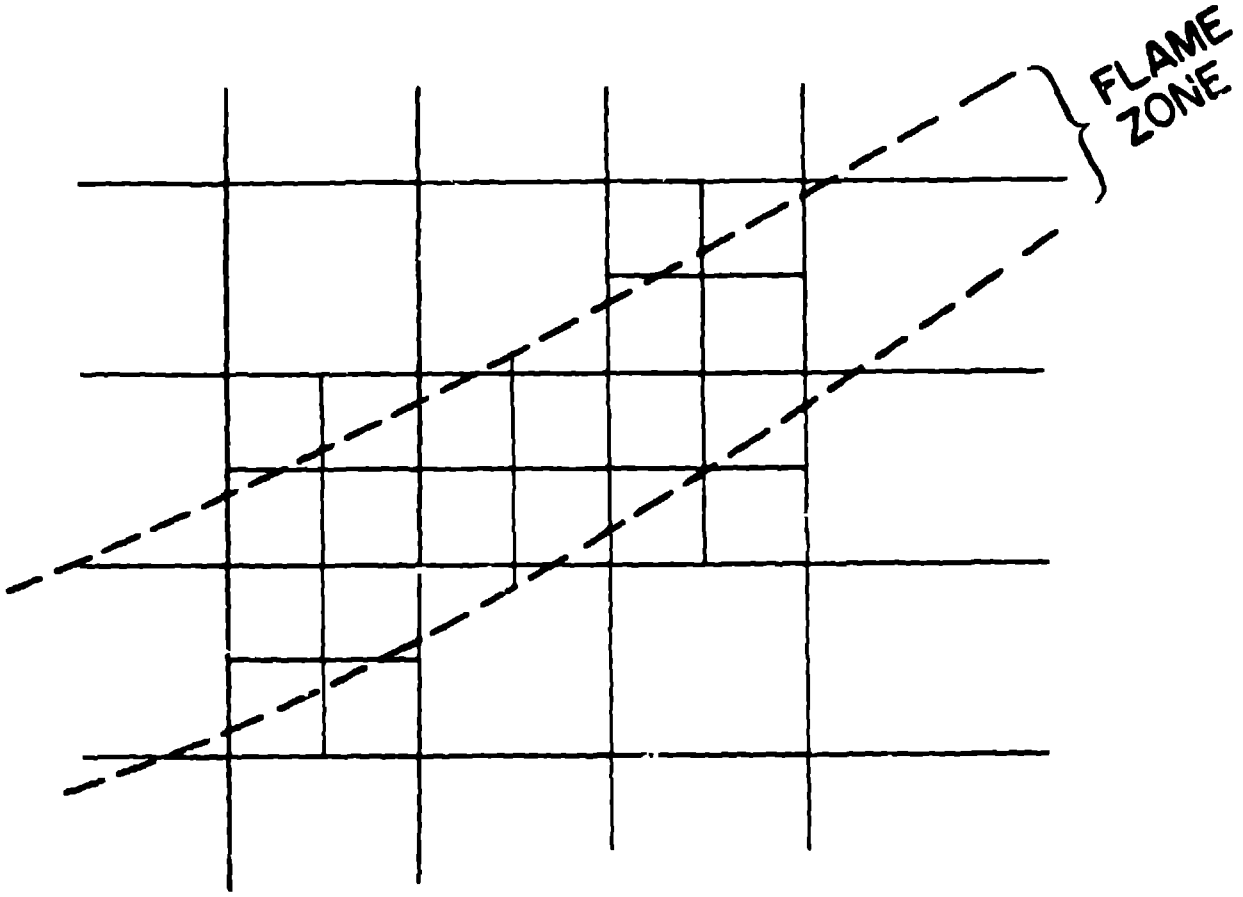
FLAME
ZONE

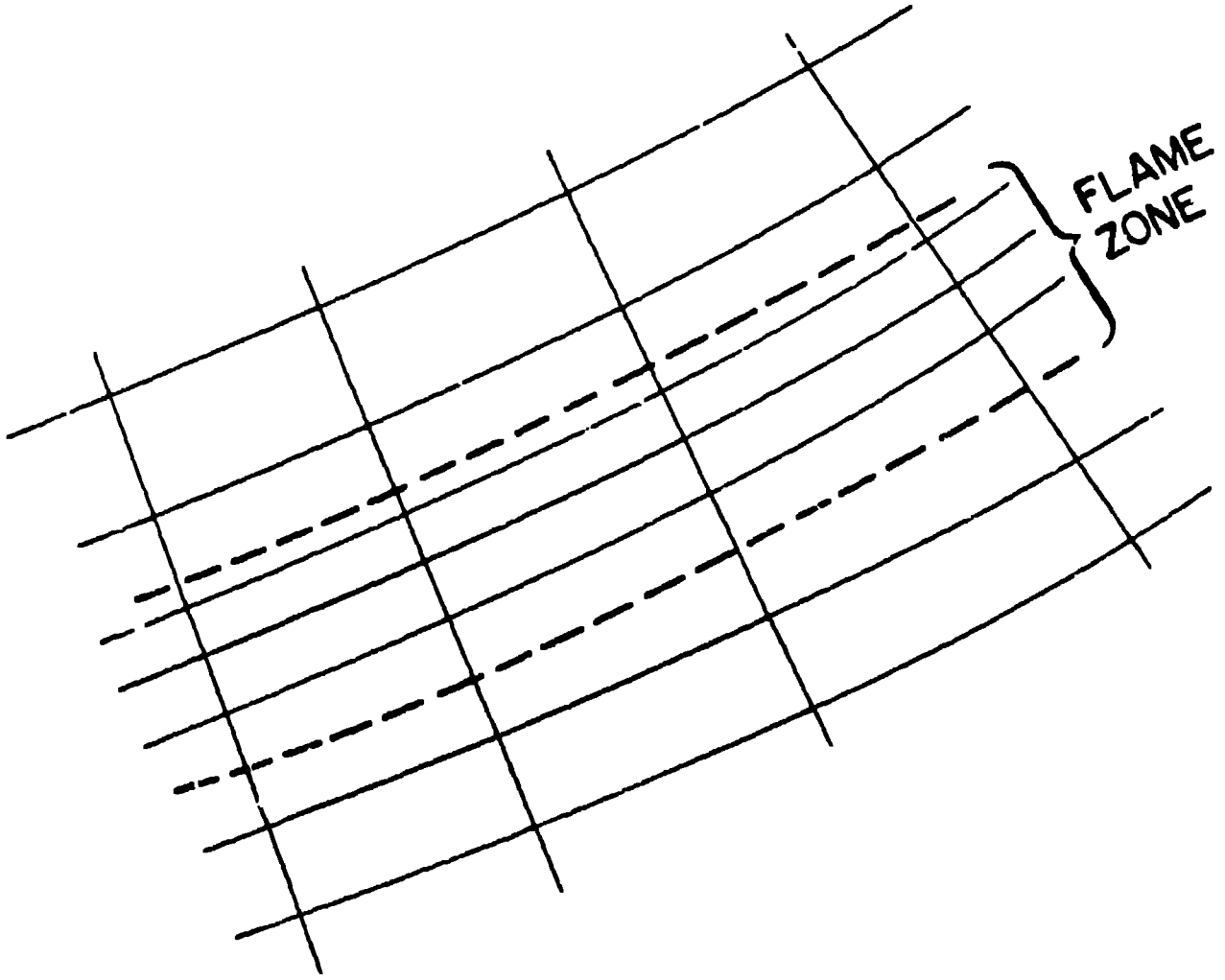
FLAME
ZONE

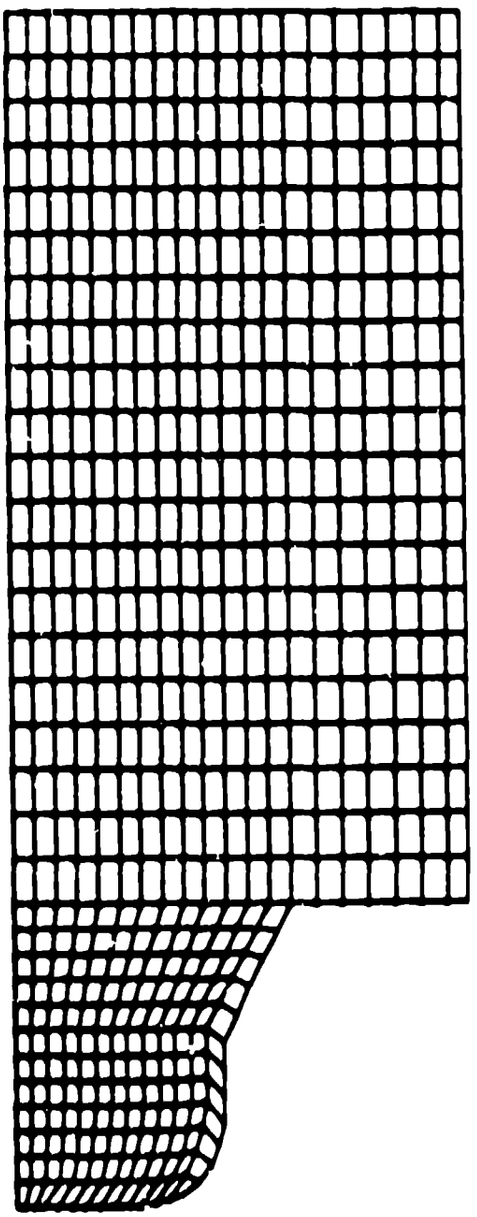

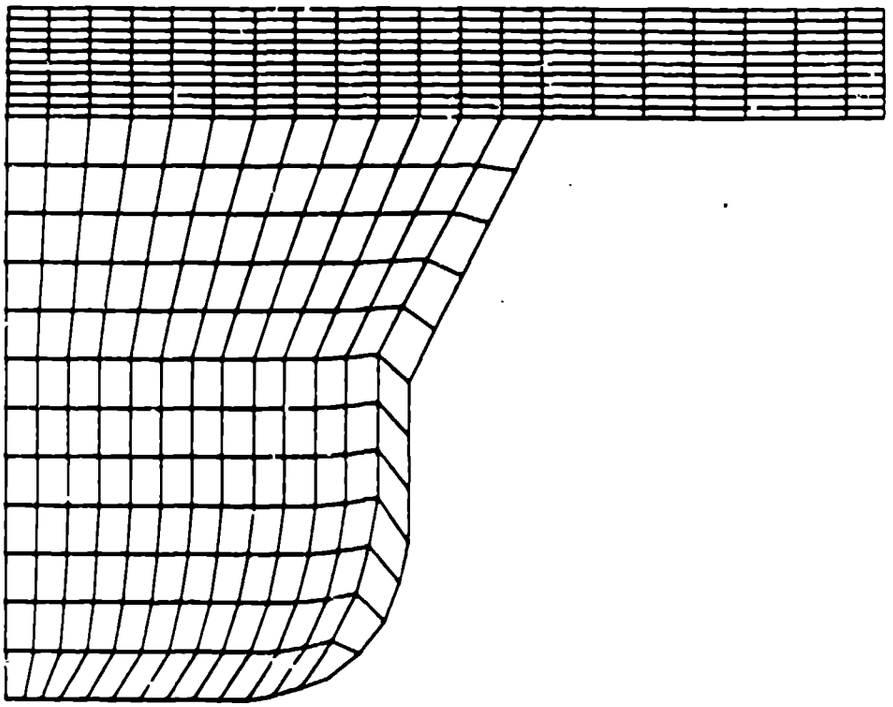

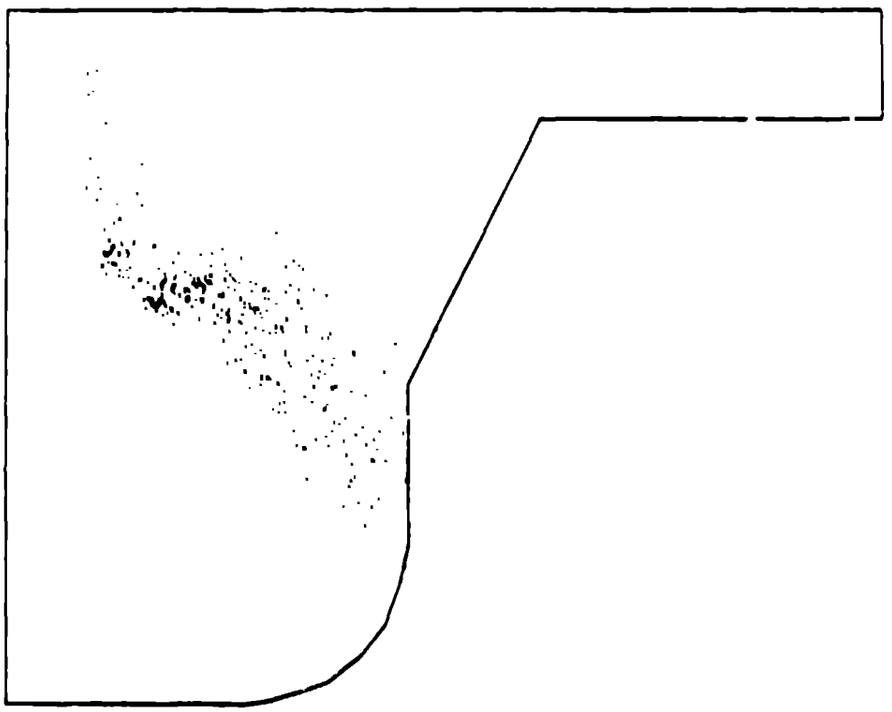

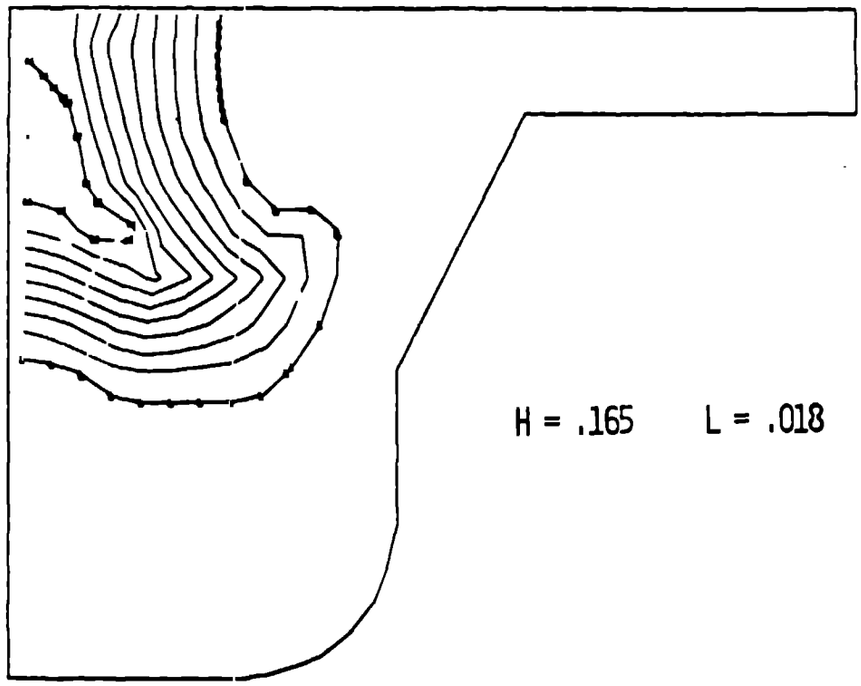
H = .165
L = .018

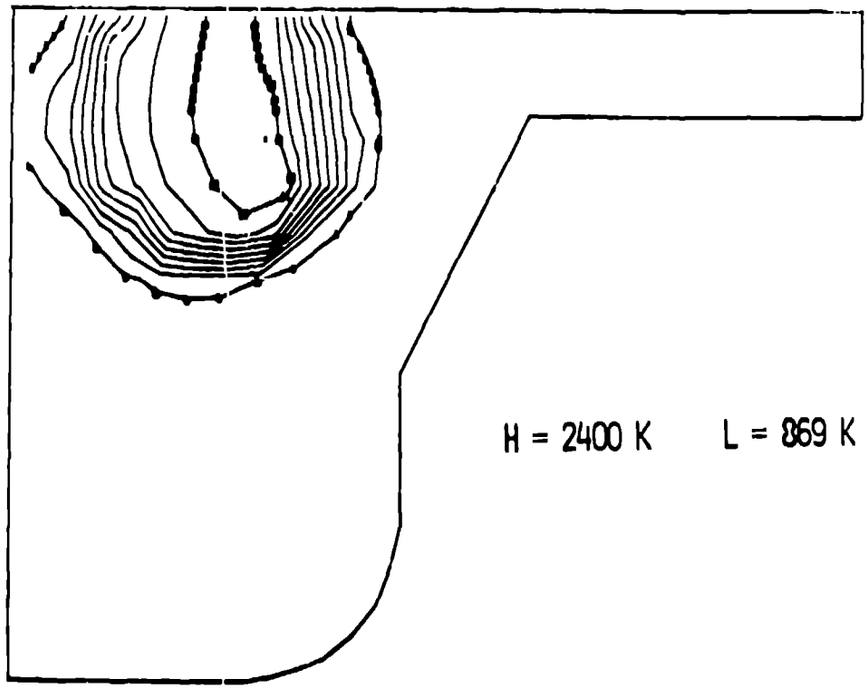
H = 2400 K
L = 869 K

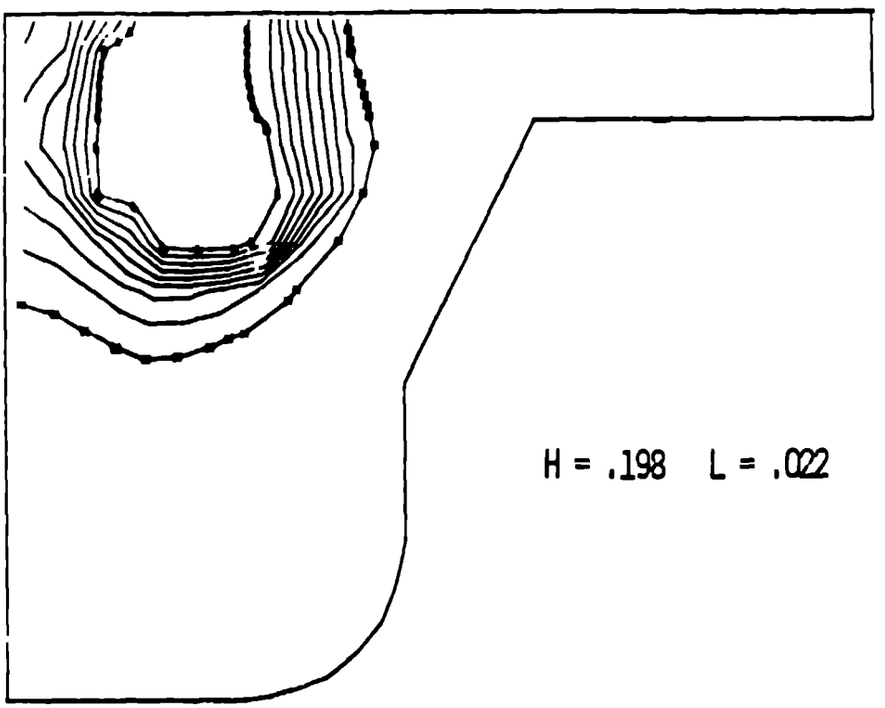
H = .198 L = .022

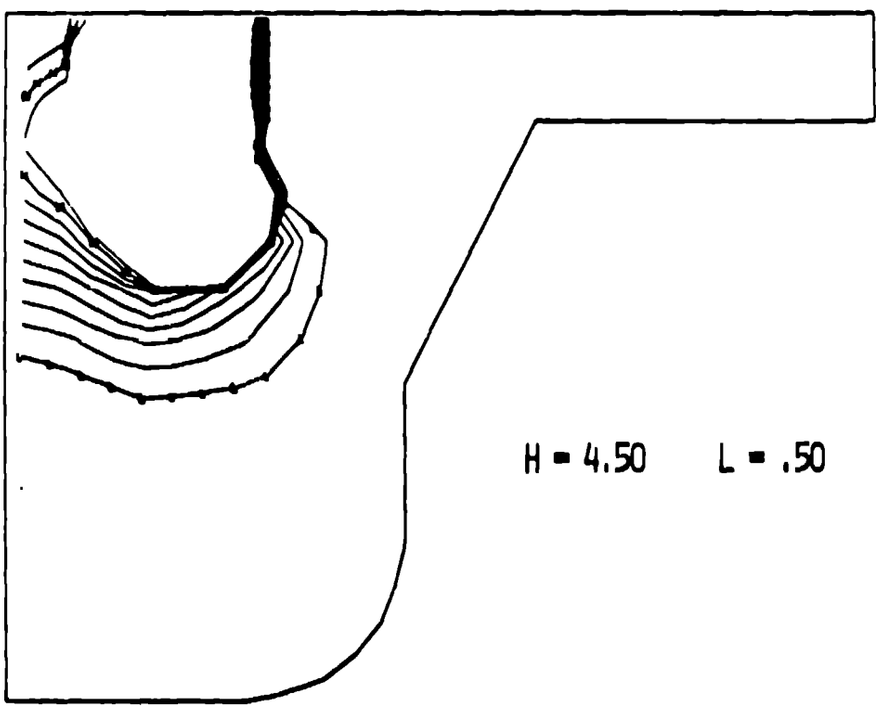
H = 4.50 L = .50